Scanning tunneling microscope with continuous flow cryostat sample cooling

Stefan Behler,[a] Mark K. Rose,[b] James C. Dunphy, D. Frank Ogletree, and Miquel Salmeron[c]
Materials Sciences Division, Lawrence Berkeley National Laboratory, University of California, Berkeley, California 94720

Claude Chapelier
Département de Recherche Fondamentale sur la Matière Condensée, CEA/Grenoble, 38054 Grenoble Cedex 9, France

(Received 7 October 1996; accepted for publication 5 March 1997)

We have constructed an ultrahigh vacuum scanning tunneling microscope (STM) for operation in the temperature range 20–300 K. The design consists of a vibration isolated sample holder mounted on a continuous flow cryostat. By rotation and linear motion of the cryostat, the sample can be positioned in front of various surface preparation and analysis instruments contained in a single vacuum chamber. A lightweight beetle-type STM head is lowered from the top onto the sample by a linear manipulator. To minimize helium convection in the cryostat, the entire vacuum system, including a liquid helium storage Dewar, can be tilted by a few degrees perpendicular to the cryostat axis, which improves the operation. The performance of the instrument is demonstrated by atomically resolved images of the Pd(111) surface and adsorbed CO molecules. © *1997 American Institute of Physics.* [S0034-6748(97)02806-2]

I. INTRODUCTION

Ever since the invention of scanning tunneling microscopy[1] (STM), it has been desirable to perform experiments at temperatures other than ambient, e.g., at cryogenic temperatures. As atomic diffusion processes and thermal fluctuations are negligible, imaging at cryogenic temperatures opens up a wide new range of experiments. Interesting surface and bulk properties have been investigated, including physisorption[2] (of atoms and molecules) at metastable sites, superconductivity,[3] charge density waves[4] and structural phase transitions.[5]

The difficulty in designing a cryogenic STM is combining good thermal contact to a liquid helium reservoir with vibration isolation of the instrument. Various designs, mostly based on the use of bath cryostats,[6,7] have been reported. The entire STM is suspended by springs and is coupled to the bath by helium exchange gas, soft copper braids or by precooling in direct contact (prior to the experiment). The advantage of this design is the high thermal stability, as thermal expansion coefficients drop with temperature and piezoelectric creep is negligible below 100 K. Furthermore, the cold instrument and the chamber walls act as cryopumps and therefore provide excellent vacuum conditions. On the other hand, most of these instruments operate at a fixed cryogenic temperature, and the cool down/warm up process takes a considerable amount of time (several hours). Therefore, these instruments are limited to experiments that do not involve rapid sample temperature cycling or imaging at variable temperature. To overcome this limitation, a bath cryostat STM can be equipped with a sample heater.[7]

In this article, we describe the construction of an ultrahigh vacuum (UHV) STM of another design that allows heating and cooling of the sample only (some K/s). The sample is imaged with a STM that operates around ambient temperature but can also be studied by other surface analytical tools *in situ.* Cooling down to 20 K is done by a liquid helium continous flow cryostat. To avoid transmission of cryostat vibrations, the sample is mounted on a vibration isolation stage and coupled to the cryostat by soft copper braids. Bott, Michely, and Comsa[8] have also independently developed a STM based on a similar approach. Our vibration isolation stage employs a unique elastomer O-ring suspension, which takes advantage of the soft bending deformation of the elastomers. The noise attenuation of the vibration isolation stage is demonstrated by comparing the noise level with and without elastomer O-ring suspension. This instrument is capable of atomic resolution on a close-packed metal surface at temperatures down to 20 K.

II. INSTRUMENT DESIGN

A. UHV system

The entire instrument is mounted onto a rectangular steel frame that sits on four air damped legs[9] for vibration isolation from the building. The main components of the system are attached to a smaller frame that rests on an axle held by the larger frame. This smaller frame can be tilted on this axle a few degrees from horizontal to avoid convection currents within the cryostat; see Sec. II B. Figure 1 shows a side view of the UHV system and its tilting axis.

The design consists of a continous flow cryostat (~100 cm long) on a differentially pumped rotary flange attached to the main UHV chamber with a bellows. A sample holder is mounted onto a vibration isolation stage at the end

[a]Present address: ESEC SA, Hinterbergstr. 32, CH-6330 Cham, Switzerland.
[b]Also at the Dept. of Physics, University of California, Berkeley, CA 94720; Electronic mail: mrose@stm.lbl.gov
[c]Author to whom all correspondence should be addressed.

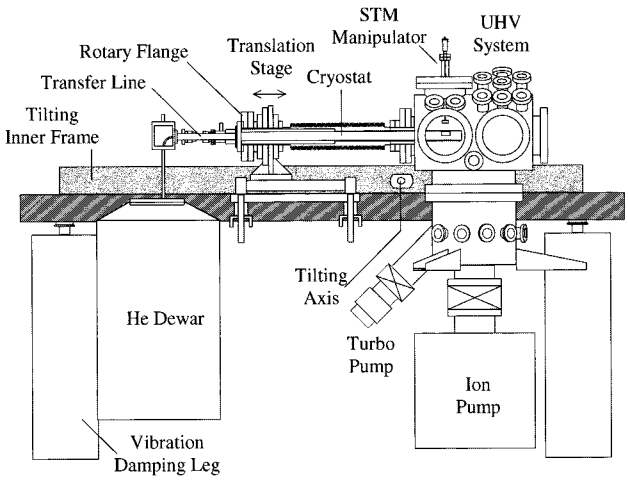

FIG. 1. Side view of the UHV STM system. The sample is cooled by a continuous flow cryostat that is mounted to a translation stage, which allows for rotation and translation of the sample. The entire system is supported by air-damped legs and can be tilted on an axle to avoid helium convection in the cryostat.

of the cryostat. Thus, by rotation and linear on-axis translation of the cryostat, the sample can be positioned in front of various surface preparation and analysis instruments contained in a single UHV chamber. Liquid helium for operating the cryostat is provided by a 30 L storage Dewar[10] mounted on the inner frame. A vacuum shielded transfer line connects the Dewar to the cryostat. The transfer line remains stationary when the cryostat is translated for sample positioning.

Two clusters of instruments are arranged around the horizontal axis of the cryostat. The components employed for sample preparation include an Auger electron spectroscopy (AES) system,[11] a differentially pumped ion sputter gun,[12] gas dosers and a mass spectrometer.[13] Adsorbate reconstructions on the sample surface can be investigated by a rear view low energy electron diffraction (LEED) system. The STM head is a stand-alone ''beetle'' type[14,15] design. It is mounted on an 8 in. flange and lowered onto the sample holder by a linear (vertical) manipulator. A rotary feedthrough on the same flange is used to position a tungsten electrode underneath the STM tip for field emission cleaning. The system is pumped by a turbomolecular pump,[16] an ion getter pump[17] and a titanium sublimation pump. During STM operation, the turbomolecular pump is turned off to eliminate vibrational noise caused by the spinning of the rotor (1 kHz).

For STM experiments, the STM head is decoupled from the vertical manipulator and rests on the sample holder by gravity. In addition to the vibration isolation stage described below, vibrations transmitted from the chamber to the cryostat are attenuated as much as possible. Three concentric Viton seals (differentially pumped) mechanically isolate the cryostat from the bellows. Additional vibration damping of the free end of the cryostat is provided by six damping arms connected to the chamber wall. The liquid helium transfer line mounts onto the cryostat with only two Viton rings in a quick flange connector. It is precisely aligned with the cryostat such that the 90 cm long transfer line does not touch the inner wall of the cryostat. The alignment is checked by measuring the electrical resistance between transfer line and cryostat.

B. Continuous flow cryostat

The continous flow cryostat is specially designed for this application to provide sufficient cooling with a minimum amount of helium flow vibrations; see Fig. 2. It employs two return paths for the helium: one within the transfer line for cooling the radiation shield, and the other the main path for cooling the cryostat. The cryostat is constructed from several layers of thin-walled stainless steel tubes to reduce its thermal conductivity. Liquid helium arrives through the center vacuum insulated and superinsulated tube inside the transfer line. It passes through a sintered copper filter[18] that disrupts large gas bubbles to give a smoother flow; the filter also keeps the hole of the adjoining needle valve clean. Some helium gas returns from this point through an outer layer of the transfer line to cool a radiation shield around the center tube. As mentioned above, the transfer line does not touch the inner wall of the cryostat except for the quick connector on the rotary flange side. Thus any vibration caused by helium flowing inside the *transfer line* should not affect the STM. Furthermore, the transfer line can be kept at liquid helium temperature while the cryostat is operated at a higher temperature.

The liquid helium needed for cooling the cryostat passes through a needle valve that adjusts the helium flow rate to the cryostat. It is externally controlled by moving the outer tube relative to the rest of the transfer line. As helium evaporates in the process of cooling the sample holder, cold gas returns through a second sintered filter and a helical heat exchanger (copper) until it leaves the cryostat through an exhaust port. Both the transfer line and cryostat helium flow rates are monitored by active flow controllers.[19] The cryostat temperature is monitored by a silicon diode[20] attached to the end of the cryostat. It is clamped between two sapphire plates to avoid overheating during electron beam heater operation (see below).

The space between the transfer line and the inner wall of the cryostat is a closed volume filled with helium. When the cryostat is leveled, the difference in density of cold helium gas on the right and warm gas on the left causes convection currents within this volume. To minimize these currents, the entire UHV system can be tilted by a few degrees, which improves the performance of the cryostat. At a flow rate of 15 slm (standard liters helium gas per minute) through the cryostat exhaust and 5 SLM through the transfer line exhaust, a cryostat temperature of 8 K can be reached when the cryostat is leveled. Tilting the system by 2.5° results in a lower temperature of 6 K; any further tilting has no effect. The initial cooling of the entire cryostat from 300 to 20 K takes $\sim$60 min and consumes 3 L of liquid helium. During operation, the consumption is $\sim$1–1.5 L/h.

Vibration damping of the free end of the cryostat is provided by six thermally insulating damping arms. They are attached to the cryostat by two rings with spring-clamped Vespel[21] ball bearings to allow for linear motion. Vespel was chosen for its excellent friction properties, high thermal resistance and tolerance of high bakeout temperatures. The

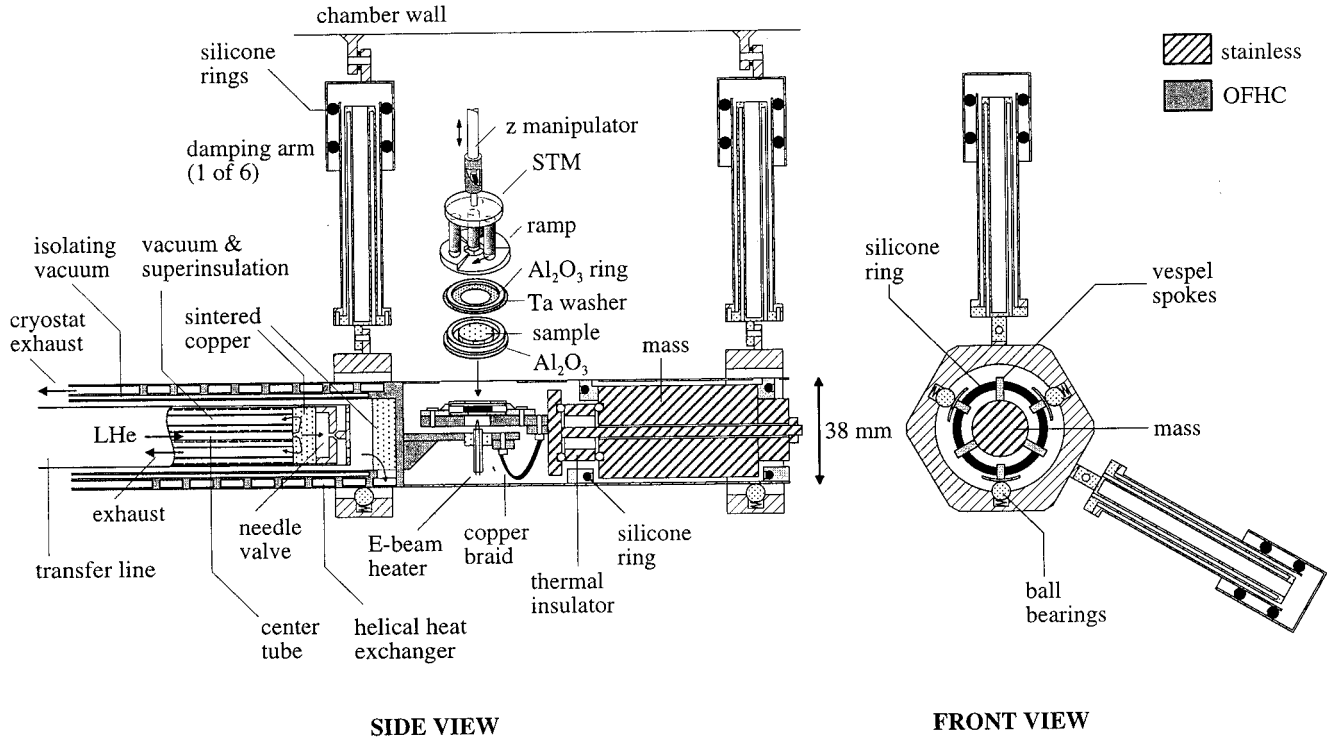

FIG. 2. Cut-away side and front views of the continous flow cryostat. The liquid helium transfer line is aligned within the cryostat to give a clearance of 1 mm on each side. The arrows inside the cryostat show the helium flow. The vibration isolation sample holder stage consists of a heavy stainless steel mass supported by O rings. The front view (on the right) shows a section through the cryostat at the right set of damping arms (one damping arm, 120° from the other two, not shown for clarity). By bending the O rings, the mass can move with respect to the cryostat, thus giving a resonance frequency well below 100 Hz.

arms are made of Vespel and stainless steel, and are folded back onto themselves to increase their effective length and thermal resistance. They are connected to the chamber wall through silicone O rings[22] clamped inside a cylinder.

C. Vibration isolation sample holder stage

The sample holder stage is an important part of the UHV system as it provides cooling and heating of the sample, as well as isolation from environmental and helium flow noise. Figure 2 shows cutaway side and front views of the assembly. Silicone elastomers[22] are employed for vibration isolation. Elastomers exhibit viscoelastic properties[23] only in a limited temperature range that is, in general, not compatible with cryogenic applications. The vibration isolation stage was therefore designed in such a way that the elastomers are thermally decoupled from the cryostat. Silicone rubber (containing Si, O, H and C) was chosen as it possesses excellent resistance to temperature extremes of up to 370 °C and is flexible down to −114 °C.

The sample holder is mounted on a copper support plate connected to a heavy stainless steel mass of cylindrical shape (~300 g). Two silicone O rings (30 mm diameter, 3 mm thickness) support the mass. They are attached to the cryostat wall (stainless steel) and are held by Vespel spokes for thermal insulation. This geometry takes advantage of the soft bending deformation of the O ring, compared to the stiffer compression deformation. The resonance frequencies of the mass held by the O rings are in the range of 20–80 Hz.

The thermal link between sample and cryostat is established by two copper braids. Good thermal conductance and softness of the braids is ensured by annealing in vacuum (10^{-4} mbar) with an infrared heater for 1 h at 400 °C. Each braid is made from single 0.08 mm oxygen-free high-conductivity (OFHC) wires, with a length of 40 mm and a total cross section of 1.5 mm. The braids are hard soldered (silver solder) to copper mounting blocks that are firmly screwed to the cryostat on one side and to the copper support plate on the other. In order to keep the solder from wetting the braid, the braid is firmly crimped with thin copper sleeves on each side and then soldered into the mounting block.

A thermal insulator between the mass and the copper support plate reduces the heat load on the cryostat and keeps the elastomers from getting cold. It consists of a stainless steel ring pressed against the support plate by three glass balls and against the mass by three Vespel balls. We found that, during cryostat operation, the temperature of the O rings does not drop below −10 °C. The insulator also decouples the O rings and the cryostat from the sample when the latter is being heated.

The sample is located below a 9 mm hole in the ramp and 2 mm below the top. It is electrically isolated from the support plate. The sample is sandwiched between a tantalum disk on top (underneath the ramp), and an Al_2O_3 ring on the copper support plate on the bottom. The ramp is clamped onto the copper support plate by four stainless steel screws.

The change in distance between the sample and the top of the ramp by thermal contraction during cooling is less than 0.05 mm. We verified this by comparing the STM head orientation with respect to the ramp at different temperatures when the tip is in tunneling.

An electron bombardment heater is mounted on the cryostat behind the vibrationally isolated sample. This arrangement allows heating of the sample up to 1000 °C without mechanical contact to the 1 mm copper wires needed for operating the heater. It consists of a 0.2 mm tungsten wire filament insulated by Al_2O_3. The sample temperature is measured by an attached type E thermocouple (NiCr/CuNi). A third wire is used for biasing the sample and grounding it during electron beam heater operation. Type E thermocouples are recommended as the most useful standard thermocouple type for cryogenic temperature measurements.[24] The thermocouple is referenced to liquid helium to reduce offset errors, as it has a sensitivity (Seebeck coefficient) of only 8.5 μV/°C at 20 K. The thermovoltage is amplified by a gain 100 chopper stabilized intrumentation amplifier with 1 μV input offset.[25]

At a cryostat temperature of 6 K, a minimum sample temperature of 20 K is reached. For STM experiments at variable temperatures, we achieve sample temperatures in the range 20–80 K by adjusting the helium flow rate in the cryostat. Higher temperatures are accomplished by radiation from the W filament behind the sample. During STM experiments at cryogenic temperatures, the sample surface can be cleaned from physisorbed contaminants (residual gas) by flashing it to 500 K (or higher) for a few seconds. The sample then cools down to 20 K in ~3 min.

Although in this article we present only STM experiments in the range 20–25 K, we have operated the instrument at sample temperatures up to 80 K. The sample was first cooled to 20 K, then the helium flow rate in the cryostat was reduced. Stable temperature was achieved after 30 min. The noise and drift performance of the instrument was comparable to experiments at 20–25 K. Above ~80 K, the very low helium throughput and associated long time constant make temperature stabilization by flow control impractical. To achieve more robust temperature control, helium flow cooling must be balanced by active heating. Although the W filament can be employed to radiatively heat the sample, warming of the filament support and the sample holder stage by thermal conduction from the white hot filament causes excessive outgassing. Currently, we are working to modify the alumina washer under the sample to incorporate a loop of Chromel wire for direct resistive heating.

D. STM

The STM is based on the ''beetle'' design inspired originally by Besocke. [14] It consists of the STM head and a helical molybdenum ramp attached to the sample holder. The head is a copper disk (2×20 mm) onto which four parallel piezoelectric tubes[26] are soldered. The center tube holds the STM tip and is used for scanning. The three outer tubes have sapphire balls glued to the end.[27] They function as legs, each resting on one of the three segments of the helical ramp. Each ramp segment has a height of 0.5 mm and covers an angle of 120°. By applying appropriate voltage pulses to the electrodes of the piezoelectric legs, the STM head can be either translated (x/y direction) or rotated with respect to the ramp. By rotating the STM head, the tip is approached towards or retracted from the sample. This motion is generated by sawtooth-like voltage pulses which cause the sapphire balls to stick or slip against the ramp depending on the speed of the leg.

A linear (vertical) manipulator holds the STM head. When not in use, the STM hangs from a horizontal 0.7 mm thick CuBe wire hooked into two asymmetric V-shaped holes cut into the opposite sides of a tube. The weight of the head pulls it to the bottom of the holes, rotating it to a specific angle. At this angle, the legs are centered over the top of the ramps. As the head is lowered onto the ramp, it decouples from the manipulator when the CuBe wire is no longer touching the sides of the V-shaped holes. The STM head is connected by 11 Kapton-insulated 0.08 mm copper wires.[28] The tip wire runs inside the stainless steel manipulator tube for electrical shielding. The temperature of the STM head is measured by a silicon diode. Even after sitting on the ramp for several hours of cryostat operation, the temperature of the copper disk does not drop below −20 °C. After ~2 h, the lateral drift of the STM tip with respect to the sample is ~5–10 Å/min (25 K).

A Burr Brown OPA 128 operational preamplifier with a 10^8 Ω feedback resistor is used as tunnel current amplifier outside the vacuum chamber. A digital signal processor[29] (DSP) controls a four channel 16-bit analog to digital converter (ADC)/digital to analog converter (DAC) and a 16 channel 12-bit DAC with 40 kHz sampling rate. It generates the scan signals and provides integral feedback for constant current STM operation. The DSP code performs an integration of the tunneling current in such a way that the tip z position is given by $z(t)=G\int \ln(I/I_0)dt$, where I and I_0 are the actual tunnel current and the setpoint. The gain G is typically 100–1000 nm/s. The outputs of the 12-bit and 16-bit DACs are scaled and summed to provide coarse and fine control of the tip position. Apex PA88 high voltage amplifiers (bandwidth 40 kHz, gain 10, noise 0.1 mV peak-to-peak with inputs connected) are used to provide ±100 V for driving the piezoelectric actuators. Modified RHK STM software[30] serves as an interface to the DSP.

III. TEST RESULTS

We have tested the instrument by performing various noise measurements, imaging the Pd(111) single crystal surface and adsorbed CO molecules. Prior to the experiments, the Pd sample surface was cleaned by sputtering and annealing to remove sulfur impurities. Sputtering was done with 1 keV Ar^+ ions (2 μA cm^{-2}) at 500 °C for 15 min, while the subsequent anneal was done for 10 min at 500 °C. Carbon impurities were removed by introducing 10^{-7} mbar oxygen at 500 °C for 1 min.

The STM tip is made from 0.25 mm polycrystalline $Pt_{90}Rh_{10}$ or W wire. $Pt_{90}Rh_{10}$ tips are electrochemically etched in a molten (~350 °C) solution of 20% NaCl and 80% $NaNO_3$ by applying +2.3 V dc between the tip and a Pt counter electrode. W tips are electrochemically etched in a

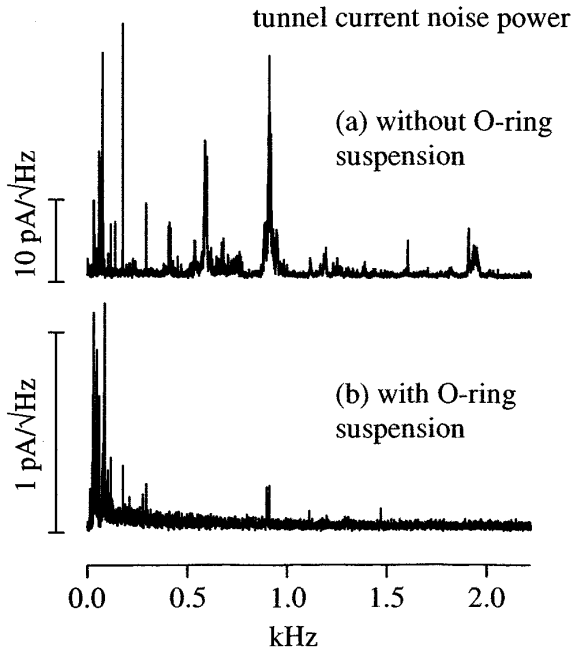

FIG. 3. Comparision of tunnel current noise spectra (a) without O-ring suspension (sample holder mounted directly on the cryostat) and (b) with O-ring suspension (sample holder mounted on vibration isolation stage). Both spectra were acquired at low temperature with a helium flow rate of 10 slm in the cryostat and 2 slm in the transfer line, I_T=1 nA, V_{sample}=500 mV, and feedback gain at minimum (30 nm/s).

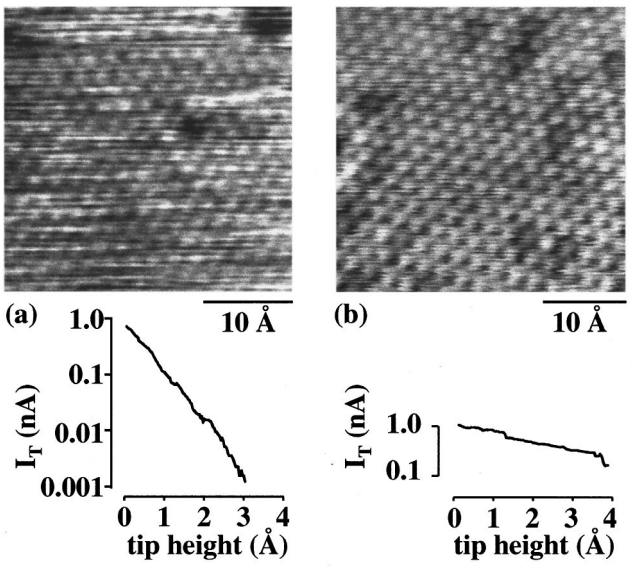

FIG. 4. Atomic resolved images of the Pd(111) surface acquired with a clean and a dirty W tip. The tunnel gap is characterized by I-Z spectroscopy data shown below the STM images. (a) In the case of the clean W tip, the apparent atomic corrugation is 0.02 Å. Note that the tunneling current drops by about one order of magnitude for each Å (I_T=1 nA, V_{sample}=80 mV, ϕ=4.5 ± 0.5 eV, 20 K). (b) A dirty tunneling gap is characterized by a weaker I-Z dependence. The corrugation in the STM image is 0.4 Å (I_T=1 nA, V_{sample}=500 mV, ϕ = 0.2 eV, 25 K). A few ''darker'' atoms can probably be assigned to carbon substituting Pd atoms in the surface layer.

KOH solution. The tip is cleaned in vacuum by positioning the tungsten field emission electrode ~1 mm underneath it (see Sec. II A). At an electrode potential of 1.5–2.5 kV, an emission current of 1 μA produces a sufficiently clean tip.

A. Noise performance

The noise attenuation of the vibration isolation stage is demonstrated in Fig. 3 by comparing the noise level with and without elastomer O-ring suspension. Tunnel current noise measurements were performed during STM experiments at 25 K on the clean Pd(111) surface using a W tip. The apparent barrier height ϕ=4.5 ± 0.5 eV derived from I-Z spectroscopy indicated a clean vacuum gap.[31] This is important for reliable noise measurements, as a ''dirty'' tunnel gap (ϕ=0.1–0.5 eV) reduces the noise significantly, apparently due to mechanical contact between tip and sample. Figure 3(a) displays the noise spectrum with the sample holder mounted *directly* on the cryostat, e.g., without elastomer O-ring suspension. It shows vibrations of the cryostat excited by the helium flow. For comparison, the noise spectrum in Fig. 3(b) was measured with the elastomer O-ring suspension in place. The spectrum was measured under similar conditions as in Fig. 3(a). Figure 3(a) clearly reveals that vibrations <100 Hz are attenuated by one order of magnitude, whereas >100 Hz the attenuation is two orders of magnitude or higher. A similar finding was already reported by Bott *et al.*[8]

B. Atomic resolution on Pd(111)

One of the biggest challenges for a STM system is to resolve the vertical atomic corrugation on a close-packed metal surface. We used W and $Pt_{90}Rh_{10}$ tips to image the Pd(111) surface at low temperature and characterized the tunneling gap by I-Z spectroscopy. Unexpectedly large atomic corrugations have often been observed by STM in the past. In many cases, this is believed to be due to a mechanical interaction between tip and sample.[32] We again observed this phenomenon of a wide range of corrugations when using W tips, as shown in Fig. 4. Large corrugations were accompanied by unexpectedly small barrier heights as derived from the z dependence of the tunneling current. Clean W tips (ϕ = 4.5 ± 0.5 eV) gave a corrugation on the order of 0.02 Å (peak-to-peak) [Fig. 4(a)]. Corrugations in the range of 0.2–0.5 Å were observed when the gap was ''dirty'' and showed an apparent barrier height of ϕ=0.1–0.5 eV [Fig. 4(b)]. Moreover, in these cases, the tunneling noise was significantly reduced, as already mentioned above. We believe that, in this case, mechanical contact—probably an oxide layer terminating the W tip—stabilizes the gap and enhances the contrast.

It is interesting that $Pt_{90}Rh_{10}$ tips show a somewhat different behavior. With these tips, atomic resolution on Pd(111) was only observed under clean gap conditions. Figure 5(c) shows an example of such an experiment (I-Z data not shown). Surprisingly, we observed large atomic corrugations of 0.1–0.2 Å under clean gap conditions. At this point we are not certain if the difference in apparent corrugation for clean W and $Pt_{90}Rh_{10}$ tips is systematic. We hope to clarify this in the future by further experiments.

C. Adsorbate studies

Atomically resolved images of CO molecules on the Pd(111) surface were acquired at 25 K with a $Pt_{90}Rh_{10}$ tip.

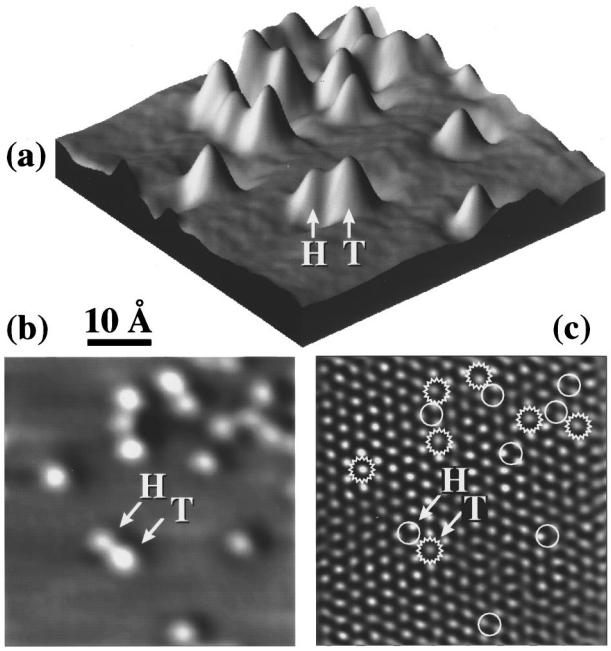

FIG. 5. (a) 3D and (b) top view STM images of CO molecules adsorbed on Pd(111) at 25 K. I_T=100 pA, V_{sample}=−50 mV, image size is 47× 47 Å, $Pt_{90}Rh_{10}$ tip. The molecules appear with two different heights, referred to as ''H'' (0.15 Å) and ''T'' (0.25 Å). The binding sites are identified as on top (T, stars) and fcc hollow (H, circles) by matching the positions of the molecules with the underlying Pd lattice in (c), an atomic resolved image of the Pd(111) surface recorded with I_T=17 nA and V_{sample}=−10 mV (Fourier filtered for clarity).

The molecules were adsorbed from the gas phase (0.06 L dosage) at 25 K with the STM tip retracted by 2 μm. Figure 5(a) shows a three-dimensional (3D) view of the molecules and Fig. 5(b) is a top view of the same image. CO adsorbs with carbon down and oxygen up,[33] and the molecules appear as cylinder-symmetrical features. We find two distinct shapes that we assign to different adsorption sites[33] on Pd(111). The molecule labeled ''T'' has the shape of a 0.25 Å high bump, whereas the molecule labeled ''H'' appears as a 0.15 Å-high bump with a shallow depletion around its base. Similar STM data were reported by Stroscio and Eigler[34] for CO on Pt(111), where it adsorbed on the on top and bridge sites. Comparison with a recent analysis of their data[35] has led us to the assumption that the molecules labeled ''T'' and ''H'' are adsorbed on the on top site and fcc hollow sites, respectively.

The underlying Pd lattice can be imaged at relatively low gap resistance (1 MΩ), Fig. 5(c). At this gap resistance, the CO molecules are moved to the side by the STM tip, therefore the adsorption site can not be identified directly. Note that, due to thermal drift and a possible tip change (caused by interaction with CO molecules), the atomic-resolved image of the Pd lattice in Fig. 5(c) does not show exactly the same part of the surface as in Figs. 5(a) and 5(b). However, we tried to match the positions of the molecules with the lattice of the Pd atoms. In Fig. 5(c) the positions of ''H'' and ''T'' molecules are indicated by circles and stars, respectively. A close match was found by placing the ''stars'' on top of Pd atoms and the circles at hollow sites. Note that the circles indicate equivalent hollow sites within the surface unit cell (one Pd atom on the left, two on the right). The unit cell contains two hollow sites (indistinguishable in the STM image), the fcc hollow site and the hcp hollow site. In the image the CO molecules occupy only one of them, most likely the fcc hollow site.[33] This experiment shows nicely that our instrument is a powerful tool for investigating low-coverage surface adsorbates with atomic resolution.

ACKNOWLEDGMENTS

This work was supported by the U.S. Air Force, Office of Scientific Research, Contract No. AFOSR-MIPR-95-0052 through the U.S. Department of Energy under Contract No. DE-AC03-76SF00098. The authors also acknowledge the Gaspar De Portola Catalan Studies Program at the University of California at Berkeley. One author (S.B.) thanks the Alexander von Humboldt Foundation of Germany, and a second author (C.C.) thanks the NATO for a fellowship and A. Benoit for helpful discussions.

[1] G. Binnig, Ch. Gerber, E. Weibel, and H. Rohrer, Phys. Rev. Lett. **50**, 120 (1983).
[2] P. S. Weiss and D. M. Eigler, Phys. Rev. Lett. **71**, 3139 (1993); P. Zeppenfeld, S. Horch, and G. Comsa, *ibid.* **73**, 1259 (1994); J. Wintterlin, R. Schuster, and G. Ertl, *ibid.* **77**, 123 (1996).
[3] H. F. Hess, C. A. Murray, and J. V. Waszczak, Phys. Rev. Lett. **69**, 2138 (1992).
[4] R. V. Coleman, B. Drake, P. K. Hansma, and G. Slough, Phys. Rev. Lett. **55**, 394 (1985).
[5] T. A. Land, T. Michely, R. J. Behm, J. C. Hemminger, and G. Comsa, Appl. Phys. A **53**, 414 (1991).
[6] R. Gaisch, J. K. Gimzewski, B. Riehl, R. R. Schlittler, M. Tsuchdy, and W. D. Schneider, Ultramicroscopy **42–44**, 1621 (1992); A. D. Kent, Ch. Renner, Ph. Niedermann, J. G. Bosch, and O. Fischer, *ibid.* **42–44**, 1632 (1992); R. R. Schulz and C. Rossel, Rev. Sci. Instrum. **65**, 1918 (1994).
[7] G. Meyer, Rev. Sci. Instrum. **67**, 2960 (1996).
[8] M. Bott, T. Michely, and G. Comsa, Rev. Sci. Instrum. **66**, 4135 (1995); S. Horch, P. Zeppenfeld, R. David, and G. Comsa, *ibid.* **65**, 3204 (1994); W. W. Crew and R. J. Madix, *ibid.* **66**, 4553 (1995).
[9] Laminar flow isolator I-2000 series, Newport Corp., Irvine, California 92714.
[10] Vapor shielded liquid helium Dewar, Cryo Industries of America, Inc., Atkinson, New Hampshire 03811.
[11] Varian 981-2707 cylindrical mirror analyzer with 10 KeV internal electron gun.
[12] Physical Electronics, Inc. (Phi) model 04-303.
[13] Dycor quadrupole mass analyzer, Ametek, Pittsburgh, Pennsylvania 15238.
[14] K. Besocke, Surf. Sci. **181**, 145 (1987).
[15] J. Frohn, J. F. Wolf, K. Besocke, and M. Teske, Rev. Sci. Instrum. **60**, 1200 (1989).
[16] Balzers turbomolecular pump model TPU 240.
[17] Varian VacIon Plus 500 ℓ/s triode ion pump.
[18] Sintered porous bronze filters, filtration rating 110, Pacific Sintered Metals, Los Angeles, California 90061.
[19] MKS type 247C mass flow controller, MKS Instrument, Inc., Andover, Massachusetts 01810.
[20] DT-470-SD-13, Lake Shore Cryotronics, Westerville, Ohio 43081.
[21] Clifton Plastics, Inc., Clifton Heights, Pennsylvania 19018.
[22] Silicone rubber, Parker Seal Group, Lexington, Kentucky 40512.
[23] M. Okano, K. Kajimura, S. Wakiyama, F. Sakai, W. Mizutani, and M. Ono, J. Vac. Sci. Technol. A **5**, 3313 (1987).
[24] Thermocouple reference tables, based on ITS-90, Omega Technologies Co., Stamford Connecticut 06907.
[25] LTC1100, Linear Technology Corp., Milpitas, CA 95035.
[26] EBL No. 2, 0.5 in. long, 0.125 in. o.d., Staveley Sensors, East Hartford, Connecticut 06108.
[27] Epo-Tek H61 single component epoxy, Epoxy Technology, Inc., Billerica, Massachusetts 01821.
[28] Scanning motion (5), translation in x (2), rotation (2), GND (1), tip (1).

[29] AT&T DSP32C digital signal processor.
[30] RHK Technology, Inc., Rochester Hills, Michigan 48309.
[31] J. A. Stroscio and W. J. Kaiser, *Scanning Tunneling Microscopy* (Academic, Boston, 1993).
[32] M. Salmeron, D. F. Ogletree, C. Ocal, H.-C. Wang, G. Neubauer, W. Kolbe, and G. Meyers, J. Vac. Sci. Technol. B **9**, 1347 (1991).
[33] H. Ohtani, M. A. Van Hove, and G. A. Somorjai, Surf. Sci. **187**, 372 (1987).
[34] J. A. Stroscio and D. M. Eigler, Science **254**, 1319 (1991).
[35] M. L. Bocquet and P. Sautet, Surf. Sci. **360**, 128 (1996).